JACS
JOURNAL OF THE AMERICAN CHEMICAL SOCIETY



Article

# Tunable heteroaromatic sulfones enhance in-cell cysteine profiling

Hashim F Motiwala, Yu-Hsuan Kuo, Brittany L. Stinger, Bruce A. Palfey, and Brent R. Martin

*J. Am. Chem. Soc.*, **Just Accepted Manuscript** • DOI: 10.1021/jacs.9b08831 • Publication Date (Web): 27 Dec 2019

# Tunable heteroaromatic sulfones enhance in-cell cysteine profiling

Hashim F. Motiwala[†], Yu-Hsuan Kuo[†,§], Brittany L. Stinger[†], Bruce A. Palfey[‡,§], Brent R. Martin[†,§,∥,*]

[†]Department of Chemistry, [§]Program in Chemical Biology, University of Michigan, 930 N. University Ave, Ann Arbor, MI 48109. [‡]Department of Biological Chemistry, University of Michigan Medical School, 5220E MSRB III 1150 W. Medical Center Drive Ann Arbor, MI 48109, [∥]Department of Medicinal Chemistry, College of Pharmacy, University of Michigan, 428 Church St., Ann Arbor, MI 48109

**ABSTRACT:** Heteroaromatic sulfones react with cysteine via nucleophilic aromatic substitution, providing a mechanistically selective and irreversible scaffold for cysteine conjugation. Here we evaluate a library of heteroaromatic sulfides with different oxidation states, heteroatom substitutions, and a series of electron donating and electron-withdrawing substituents. Select substitutions profoundly influence reactivity and stability compared to conventional cysteine conjugation reagents, increasing the reaction rate by >3-orders of magnitude. The findings establish a series of synthetically accessible electrophilic scaffolds tunable across multiple tunable centers. New electrophiles and their corresponding alkyne-conjugates were profiled directly in cultured cells, achieving thiol saturation in a few minutes at sub-millimolar concentrations. Direct addition of desthiobiotin-functionalized probes to cultured cells simplified enrichment and elution to enable mass spectrometry discovery of >3000 reactive and/or accessible thiols labeled in their native cellular environments in a fraction of the standard analysis time. Surprisingly, only 1/2 of annotated cysteines were identified by both iodoacetamide-desthiobiotin and methylsulfonylbenzothiazole-desthiobiotin in replicate experiments, demonstrating complementary detection by mass spectrometry analysis. These probes offer advantages over existing cysteine alkylation reagents, including accelerated reaction rates, improved stability, and robust ionization for mass spectrometry applications. Overall, heteroaromatic sulfones provide modular tunability, shifted chromatographic elution times, and superior in-cell cysteine profiling for in-depth proteome-wide analysis and covalent ligand discovery.

## INTRODUCTION

First reported in 2012, methylsulfonylbenzothiazole (MSBT; **BT-1**) reacts with cysteine by a nucleophilic aromatic substitution ($S_NAr$) mechanism (**Scheme 1** and **Figure 1a**).[1] This class of electrophiles was later expanded to include more efficient oxadiazole (**OD-1**) and tetrazole (**Tz-2**) methyl sulfones (**Figure 1a**), which improve thiol blocking[2] and form stable protein-drug conjugates[2a, 3]. These heteroaromatic sulfone electrophiles show advantages over maleimide for thiol blocking and antibody-drug conjugates since they demonstrate exquisite selectivity for thiols (–SH) (i.e. no reaction with –SOH, –SNO, lysine, etc.)[2b] and form exceptionally stable, irreversible adducts[3]. In contrast to iodoacetamide and maleimide, the $S_NAr$ mechanism prevents conjugation to sulfenic acids (R–SOH), providing a useful approach for thiolate selective cysteine conjugation, particularly for thiol blocking in cysteine oxidation analysis[2b, 4].

The heteroaromatic pharmacophores are privileged structures in medicinal chemistry, commonly found in many FDA-approved drugs across diverse therapeutic applications.[5] Hence, beyond their utility as bioconjugation reagents[3, 6], similar scaffolds have also emerged in inhibitors for Glucagon-like Peptide-1 Receptor (GLP-1R)[7] and bacterial dihydrolipoamide *S*-succinyltransferase[8] as well as anti-microbial, anti-fungal, and anti-cancer activities.[9] In addition, 2-sulfonylpyrimidines have been reported as covalent stabilizers of mutant p53[10], as well as thiol-reactive inducers of redox stress for treating tuberculosis[11]. A recent picomolar potency Rho/MRTF/SRE pathway inhibitor reported an identical core scaffold to **OD-1**, substituting the methyl sulfonyl leaving group for thiopropionic acid[12]. Despite the potentially broad reactivity of these heteroaromatic sulfones, there are no systematic efforts to tune their reactivity, explore different heterocycles, evaluate distinct oxidation states, measure stability, quantify reaction rates, or expand their utility for cysteine activity/reactivity-based profiling and other proteomics applications.

**Scheme 1**

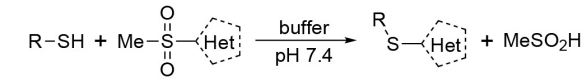


Current cysteine profiling methods use iodoacetamide-alkyne (IAM-alkyne) labeling in soluble cell or tissue homogenates[13]. The TOP-ABPP (Tandem Orthogonal Proteolysis – Activity-Based Protein Profiling)[14] approach enables site-specific analysis of cysteine accessibility and reactivity[13b], redox modification status[15], and/or covalent engagement[16]. Cells homogenates are treated with differing concentrations of iodoacetamide-alkyne to identify exceptionally reactive cysteines (enzyme active site, redox sensitive sites) that resist dilution effects. After click chemistry labeling with biotin affinity tags, a control and an experimental sample of modified cysteine-peptides are enriched and released (either chemically or proteolytically) for analysis by mass spectrometry, resulting in comparative ratios reflecting site-specific cysteine reactivity/occupancy. These technically challenging conjugation and enrichment steps can introduce significant variance. These sources of error are mitigated by introducing isotopic affinity tags, stable isotope labeling with amino acids in cell culture (SILAC), or other

quantitative labeling methods[17]. Once optimized, this approach provides proteome-wide measurements of cysteine engagement by covalent inhibitors or inhibitor fragments[16, 18], greatly enhancing their preclinical development. Despite a wide number of successes *in vitro*, the TOP-ABPP approach is constrained by weak iodoacetamide-alkyne reactivity, which limits rapid in-cell capture of accessible thiols.

Here we report a systematic exploration of heteroaromatic sulfone electrophiles, revealing general rules for tuning electrophilicity, both through sulfur oxidation and electronic substitutions that reproduce across different scaffolds. We report the first application of heteroaromatic sulfones in bottom-up proteomics applications. Optimal scaffolds were selected for desthiobiotin conjugation, allowing robust in-cell conjugation and site-specific mass spectrometry analysis of accessible and/or reactive cysteines in their native cellular environment. Overall, these efforts complement iodoacetamide-based cysteine profiling to measure an orthogonal subset of cysteine peptides. Such chemical and physical complementarity establishes heteraromatic sulfones as a distinct class of synthetically accessible, tunable covalent probes.

## EXPERIMENTAL METHODS

**Reaction rate determination**. Reactions were performed in 20% acetonitrile (ACN) in Dulbecco's phosphate buffered saline (DPBS) (2X) at pH 7.5 supplemented with 5 mM EDTA. Measurements were performed using an Agilent Cary 100 UV-Visible spectrophotometer. The compound (30 μM) was quickly mixed with *N*-acetyl-L-cysteine methyl ester at five different concentrations, depending on the relative absorbance. A UV-visible absorbance spectrum was acquired at the most responsive wavelength for time-dependent rate measurements. For more reactive electrophiles, a Hi-Tech Scientific KinetAsyst SF-61 DX2 stopped-flow spectrophotometer was used in single mixing mode to monitor the rapid formation of cysteine-electrophile conjugate. Pseudo first order rate constants were obtained by fitting the data using "one-phase association/decay" in a GraphPad Prism. And second order reaction rate was obtained by plotting the $k_{obs}$ at different concentrations of cysteine.

**Electrophile stability determination.** HPLC analysis was performed on Agilent 6520 Accurate-Mass Q-TOF LC/MS using a Waters C18 column (4.6 x 75 mm; 3.5 μm particle size). LC solvents were: 0.1% formic acid (FA) and 10 mM ammonium formate (AF) in $H_2O$ (Buffer A) and 0.1% FA and 10 mM AF in 90:10 ACN:$H_2O$ (Buffer B). A standard gradient (5–95% buffer B over 11 min) at 0.40 mL/min was used to analyze each electrophile (1 mM in PBS) at different time points of incubation at room temperature (0, 4, and 24 h). Area under the curve (either at 250 or 280 nm wavelength) was integrated at each time point and analyzed using Agilent MassHunter software.

**Cell and tissue lysate preparation.** HeLa cells were maintained in DMEM supplemented with 10% fetal bovine serum (FBS) and 1% Penicillin–Streptomycin under 5% $CO_2$ atmosphere at 37 °C. Cells were harvested by scraping, washed, and sonicated at 4 °C. Mouse brains (C57BL6) were dissected, frozen in liquid $N_2$, and stored at –80 °C. Tissues were later thawed on ice, dounce homogenized in DPBS (1X) and centrifuged at 3,000 x g for 5 min at 4 °C to remove debris. The supernatant was cleared by centrifugation (35,000 x g for 45 min at 4 °C) to yield the soluble proteome. Protein concentrations were measured using a DC assay (Bio-Rad).

**Electrophile profiling in mouse brain soluble proteome.** Mouse brain soluble proteome in DPBS (1X) was adjusted with appropriate amount of modified RIPA lysis buffer (pH 7.41, 50 mM Tris·HCl, 150 mM NaCl, 2 mM EDTA, 0.10% SDS) to 1 mg/mL protein. The resulting lysate (50 μg of protein in 46 μL for each sample) was treated with 1 mM TCEP (tris(2-carboxyethyl)phosphine hydrochloride) for 1 h at room temperature (rt) in dark. TCEP was removed using Vivaspin® 500 μL ultrafiltration spin column and supplemented with 3.6% DMSO to ensure compound solubility. Electrophiles (5mM) were added and incubated for 30 min at rt. **BT-5**, **BT-6**, **BT-7**, **BT-9**, **BT-10**, **OD-1**, and **TD-1** showed different degrees of insolubility. 5-TMRIA (tetramethylrhodamine-5-iodoacetamide dihydroiodide) was added to each sample and incubated for 30 min at rt (10% final DMSO content). The reaction was quenched by the addition of 5X Laemmli sample buffer, heated at ~90 °C for 5 min, and separated by 12% SDS-PAGE. Gels were visualized using the Cy3 channel on Amersham Typhoon Gel and Blot Imaging Systems. Gels were then stained with Coomassie to image protein loading using the Cy5 channel.

**Live cell alkyne-probe labeling.** HeLa cells were incubated with either DMSO, IAM-alkyne, BT-alkyne, Tz-alkyne, and OD-alkyne in cysteine-free DMEM media (without cystine, methionine, L-glutamine, and sodium pyruvate) for 45 min at 37 °C. Cell lysate was prepared and normalized to 1 mg/mL protein. Copper(I)-catalyzed alkyne-azide cycloaddition (CuAAC) reaction was performed using 50 μg of protein with a premixed solution at standard concentrations of TBTA (tris[(1-benzyl-1H-1,2,3-triazol-4-yl)methyl]amine) and copper (II) sulfate, TAMRA-azide, and sodium ascorbate for 1 h in dark. The reaction was quenched by the addition with 5X Laemmli sample buffer, heated at ~85 °C for 5 min, and analyzed by 12% SDS-PAGE. Gels were visualized using a Cy3 channel (TAMRA) and Cy5 (Coomassie) on Amersham Typhoon Gel and Blot Imaging Systems.

**Mass spectrometry analysis of labeled cysteines.** Mouse brain soluble proteome or probe-treated HeLa cell lysates (1 h treatment) in DPBS (1X) was diluted with 50 mM HEPES (4-(2-hydroxyethyl)-1-piperazineethanesulfonic acid) buffer. The sample was heat denatured at ~100 °C for 15 min followed by sonication of resulting hot cloudy solution in an ultrasonic bath for ~1–2 min at ~40 °C. The denatured sample was treated with 1 mM TCEP for 1 h at rt in dark followed by incubation with respective electrophile for 30 min. Importantly, we found TCEP reacts with IAM and most heteroaromatic sulfones, decreasing their actual concentrations by ~50% in 1 h. Next, the sample was digested with trypsin (1:20 ratio), diluted with 50 mM TEAB (triethylammonium bicarbonate) buffer (pH 8.5), and incubated at 37 °C for 18 h. The samples were desalted using an Oasis HLB SPE resin on a Water Oasis μElution 96-well plate. The peptides were eluted with acetonitrile, dried using a SpeedVac (45 °C, 5 mbar, 45 min), and stored at –80 °C prior to analysis.

For live cell labeling, samples were extracted with chloroform/methanol to remove salts and excess reagents and resuspended in 100 μL of 2 M urea in DPBS with 0.2% SDS and 88 μL of 50 mM TEAB by sonication. The solution was then digested with ~1:30 trypsin at 37 °C for 15 h, dried by SpeedVac, and resuspended in 300 μL of 1X DPBS.

For enrichment, the tryptic peptides were incubated with Pierce high capacity streptavidin agarose resin (150 μL, 50% slurry in 1X DPBS) for 4 h rotating at rt. After transfer to Bio-Rad micro Bio-Spin columns, the samples were washed 5 times with 0.75 mL of DPBS and 9 times with 0.75 mL of DI water. The peptides from each sample were eluted from the resin by incubating the resin two times with 100 μL of the elution buffer (1:1 ACN:water with 0.1% TFA, LCMS-grade) for ~5 min at rt and one time with 100 μL of the elution buffer for ~5 min at 60 °C. The total eluents (300 μL) containing the enriched peptides were concentrated on a SpeedVac.

Peptides were reconstituted in water with 0.1% TFA and analyzed by Orbitrap Fusion Lumos Tribrid Mass Spectrometer (Thermo Scientific). An Acclaim PepMap 100 C18 LC column (50 cm long x 75μm diameter x 2 μm particle size) was used. LC solvents were: 0.1% FA in $H_2O$ (Buffer A) and 0.1% FA in 80:20 ACN:$H_2O$ (Buffer B). Peptides were eluted into the mass spectrometer at a flow rate of 300 nL/min over a 120 minutes linear gradient (5-40% Buffer B from 2–95 min and then 40-90% Buffer B from 95–115 min) at 35 °C. MS data was acquired in a data-dependent mode. Full MS spectra were collected with following parameters (Orbitrap resolution: 60,000; scan range: m/z 300-1800 (400–2000 for desthiobiotin probes); AGC target: 2.0e5; maximum injection time: 50 ms). The MS2 spectra were collected with following scan parameters (Orbitrap resolution: 15,000; AGC target: 1.0e5; maximum injection time: 22 ms; isolation window: m/z 1.6; CID collision energy: 34%). Dynamic exclusion was set to 40 s with a mass tolerance of 10 ppm. The MS data was analyzed with Thermo Proteome Discoverer (V2.2.0.388) and searched against the mouse or human proteome (Uniprot) and a common list of contaminants. The precursor

mass tolerance was set at 10 ppm, fragment mass tolerance was set to 0.1 Da, and maximum missed cleavage sites was set to 1. The false discovery rate for peptides, proteins and sites identification was set to 1%. The minimum peptide length was set to five amino acids and peptide re-quantification was enabled. The minimal number of peptides per protein was set to one. Methionine oxidation, deamidation (N and Q), *N*-acetylation on a protein terminus, and modification of cysteines or other amino acids by a respective electrophile were searched as dynamic modifications.

**Western Blotting.** SDS-PAGE gels were transferred to a polyvinylidene difluoride (PVDF) membrane (75V, 2 h, ~4 °C) using a Mini Trans-Blot Cell (Bio-Rad). The membrane was washed, blocked with 4% w/v of BSA in 1X TBST, and incubated with streptavidin-Cy 8 (1:3000) in 1X TBST for 1.5 h. Primary antibody incubation (1:1000 mouse alpha-tubulin for loading standard) was performed in 4% BSA solution in 1X TBST for 2 h followed by further incubation with secondary antibody (1:4000 of Alexa Fluor 647 donkey anti-mouse) in 1X TBST for 1 h on a rotator at rt in a dark. After washings, the membrane was briefly dried in air and then imaged on Azure C600 Imager: 800 NIR channel and Cy5 channel were used for Streptavidin-Cy8 and Alexa Fluor, respectively.

## RESULTS AND DISCUSSION

**General heteroaromatic sulfones.** Heteroaromatic sulfones are validated reagents for bioconjugation, providing a platform for generation of stable, serum-resistant antibody-drug conjugates[3, 19]. In addition, **Tz-1** added to live cells prevents post-lysis oxidation of *S*-sulfenylated peroxiredoxin[2b], yet a brief (5 min) incubation with 10 mM **Tz-1** fails to block the majority of thiols in living cells[2b]. In order to more accurately quantify heteroaromatic sulfone reactivity, a UV absorbance assay was developed to monitor the rate of cysteine conjugation to different electrophiles (**Figure 1a**). NEM yielded the fastest reaction rate (1585 ± 109 $M^{-1}s^{-1}$), which proceeds >3-orders of magnitude faster than IAM (0.902 ± 0.05 $M^{-1}s^{-1}$). Heteroaromatic sulfone reaction rates were variable, where **OD-1** was ~75x faster than **Tz-1,** ~500x faster than IAM, and ~850x faster than **BT-1**.

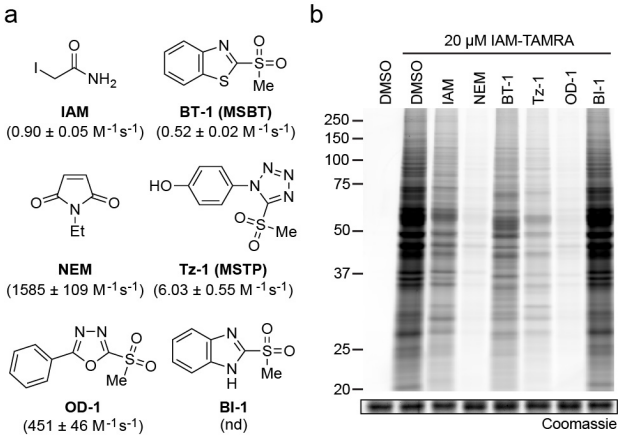


**Figure 1.** Competitive ABPP profile of cysteine electrophiles in mouse brain soluble lysate. (a) Structures and rates of cysteine electrophiles. Measured reaction rates are shown in parentheses below each electrophile. Standard deviations are derived from replicates with multi-point curve-fitting. nd = not determined. (b) In-gel fluorescence analysis of 5 mM heteroaromatic sulfone, IAM, or NEM followed by incubation and detection with 20 μM IAM-TAMRA.

To validate the proteome reactivity of this class of electrophiles, we evaluated reported heteroaromatic sulfones by gel-based competitive activity-based protein profiling (ABPP) with iodoacetamide-tetramethylrhodamine (IAM-TAMRA; 5-TMRIA) in mouse brain homogenates (**Figure 1b**). The relative efficiency of cysteine alkylation mirrored the measured reactivity trend with free cysteine (**OD-1** > **Tz-1** > **BT-1** > **BI-1**). This result conflicts with a separate report finding **OD-1** as the least efficient electrophile in cell lysates, which may reflect its marginal aqueous stability.[2b] Surprisingly, incubation with either 5 mM IAM or **BT-1** was insufficient to block all thiols, while NEM and **OD-1** saturated all sites. 4-(5-(Methylsulfonyl)-1*H*-tetrazol-1-yl)phenol (MSTP; **Tz-1**) displayed reactivity in between **BT-1** and **OD-1**, while benzimidazole methyl sulfone (**BI-1**) showed weak or no cysteine reactivity. Altogether, these findings corroborate a direct relationship between the isolated reaction rates and cysteine alkylation efficiency in complex proteomes. Clearly modulating the heterocycle immensely influences the cysteine reactivity of the heteroaromatic sulfones.

**Heteroaromatic scaffold optimization.** In order to assess the potential to tune cysteine reactivity, we evaluated the structure-activity profile across heteroaromatic scaffolds. More than 20 different heteroaromatic sulfones were synthesized, assayed by UV-absorbance kinetics, and profiled by IAM-TAMRA in-gel competitive ABPP (**Figures 2 and 3**). This analysis revealed a broad range of reactivities and provides general design rules applicable across distinct classes of heteroaromatic sulfones.

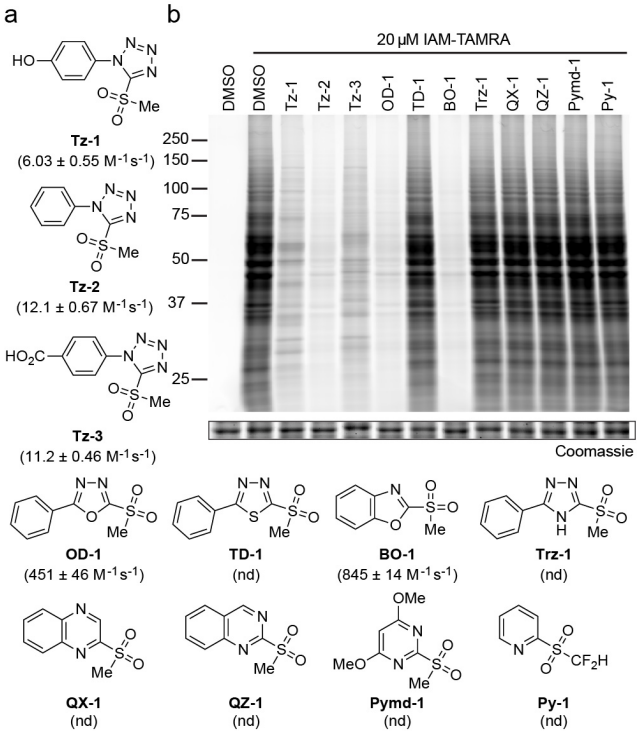


**Figure 2.** Evaluation of cysteine reactivity across different heteroaromatic scaffolds. (a) Structures of heteroaromatic methyl sulfones evaluated. Measured reaction rates are shown in parentheses below each electrophile. Standard deviations are derived from replicates with multi-point curve-fitting. nd = not determined. (b) Competitive IAM-TAMRA activity-based profiling of cysteine electrophiles (5 mM) by in-gel fluorescence.

Remarkably, replacing the sulfur atom in benzothiazole to an oxygen atom in benzoxazole (**BO-1**) increased reactivity by >1600-fold, achieving rates 2x faster than **OD-1** (**Figure 2**). Conversely, substituting the oxadiazole with a thiadiazole (**TD-1**) completely eliminated cysteine reactivity. Other five- and six-membered heteroaromatic methyl sulfones, including

phenyltriazole (**Trz-1**), quinoxaline (**QX-1**), quinazoline (**QZ-1**), pyrimidine (**Pymd-1**), and pyridine (**Py-1**), showed no significant cysteine labeling. Despite a general loss of reactivity, analogues with weak or no apparent in-gel competition may still engage select cellular targets. While not generally reactive in our assays, 2-sulfonylpyrimidines are reported to alkylate and partially rescue mutant p53 activity.[10] Clearly, subtle electronics translate to major variations in heteroaromatic sulfone reactivity, and thus imparting the capacity to derive selectivity through rational reactivity tuning.

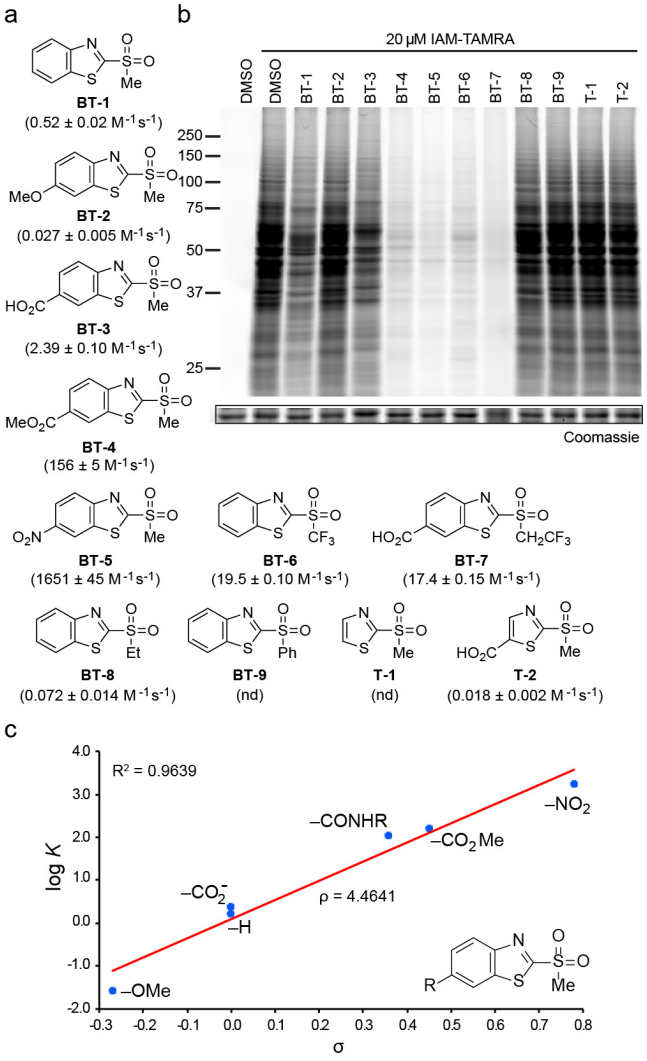


**Figure 3.** Substitutions on benzothiazoles modulate cysteine reactivity. (a) Structures of benzothiazole analogues evaluated. Measured reaction rates are shown in parentheses below each electrophile. Standard deviations are derived from replicates with multipoint curve-fitting. nd = not determined. (b) Competitive IAM-TAMRA activity-based profiling of cysteine electrophiles (5 mM) by in-gel fluorescence. (c) Hammett plot of benzothiazole derivatives.

Next, we hypothesized that substitution of an electron-withdrawing group on **OD-1** or **BO-1**, such as $–CO_2H$ on the aryl-ring, might enhance reactivity. Despite extensive efforts, neither products were stable and decomposed to corresponding hydrolysis product. Conversely, derivatives of phenyltetrazole scaffold with either an electron-donating (–OH; **Tz-1**), neutral (–H; **Tz-2**), or electron-withdrawing ($–CO_2H$; **Tz-3**) group at the *para*-position of the phenyl ring revealed little difference in rate and cysteine reactivity. Thus, not all scaffolds are as readily tunable with simple substitutions.

**Benzothiazole scaffold optimization.** Reported oxadiazole (**OD-1**) and tetrazole (**Tz-1**) scaffolds differ from the benzothiazole and benzoxazole scaffolds, where a benzene ring is directly fused to the heterocycle[2a]. Since benzoxazole compound **BO-1** was highly reactive and unstable, we sought to explore if benzothiazoles could be more effectively tuned to modulate reactivity. A small series of benzothiazole derivatives were synthesized covering a range of substituents on both the benzene ring and sulfone (**Figure 3a**). Across the benzothiazole series, subtle changes in electronics played a major role in tuning the electrophilicity (**Figure 3a-b**). For example, the electron-donating methoxy-substituted analogue (**BT-2**) was ~20-fold slower than unsubstituted **BT-1**. Electron-withdrawing substituents such as carboxylic acid (**BT-3**), methyl ester (**BT-4**), and nitro (**BT-5**) greatly accelerated the reaction rate by 5x, 300x, and 3200x, respectively. The reactivity of **BT-5** mirrored NEM in aqueous buffer, providing equivalent reactivity as the classic bioconjugation reagent. A linear Hammett plot across substituted benzothiazoles reported a positive slope ($\rho = 4.464$), validating the electronic tunability of this reactive scaffold[20] (**Figure 3c**).

We next examined if leaving group modifications could influence reactivity. To test this hypothesis, we synthesized an electron-withdrawing trifluoromethylsulfonyl analogue (**BT-6**) and a trifluoroethylsulfonyl analogue (**BT-7**). Compared to **BT-1**, fluorine substitution increased the reaction rate of **BT-6** by ~38-fold, while **BT-7** was only 8-fold faster than its corresponding non-fluorinated analogue (**BT-3**). Conversely, ethyl (**BT-8**) and phenyl (**BT-9**) sulfonyl benzothiazoles were nearly unreactive, corroborating reports that steric effects impact leaving group ability. Presumably due to the high intrinsic reactivity and instability, we were unable to synthesize a hybrid electrophile combining both the 6-methyl ester substituent on the benzene ring with the trifluoromethylsulfonyl leaving group. This again highlights a potential reactivity ceiling, where the intrinsic stability and hydrolysis requires a corresponding balance with reactivity. Finally, the minimalist thiazole methyl sulfones (**T-1** and **T-2**) showed marginal or no cysteine reactivity, establishing the importance of a benzene-fused heterocycle.

**Oxidation state profiling.** Given the tunability of both the benzothiazole scaffold and the sulfone leaving group, we next examined the influence of different oxidation states of sulfur on the reaction rate (**Figure 4a-b**). Oxidation of the 6-nitrobenzothiazole thioether to the corresponding methyl sulfoxide (**BT-10**) imparted robust cysteine reactivity, which was then further enhanced by oxidation to the sulfone (**BT-5**). A similar trend was observed with the phenyloxadiazole methyl sulfoxide (**OD-2**) and benzoxazole methyl sulfoxide (**BO-2**), where the corresponding thioethers were virtually non-reactive. Further oxidation to the corresponding methyl sulfones **OD-1** and **BO-1** enhanced the reactivity by 10-15-fold. The 6-carboxylic acid benzothiazole trifluoromethyl sulfoxide (**BT-11**) was more reactive than the 2-methylsulfonyl benzothiazole-6-carboxylic acid **BT-3**, but less reactive than the benzothiazole trifluoromethyl sulfone **BT-6**.

Further IAM-TAMRA competitive ABPP labeling at various concentrations in mouse brain homogenates confirmed the identification of several promising heteroaromatic sulfones and sulfoxides with effective thiol blocking concentrations as low as 0.10 mM (**Figure S1**). Overall, tuning the sulfur oxidation state provides a simple strategy to dial electrophilicity across

general heterocyclic scaffolds. This finding is particularly relevant as heterocyclic thioethers and sulfoxides are present in several FDA-approved drugs, including omeprazole, cefazolin, and latamoxef.[21] These drugs can potentially undergo oxidation during metabolism or due to cellular redox stress, which could impart significant reactivity to a generally inert scaffold.

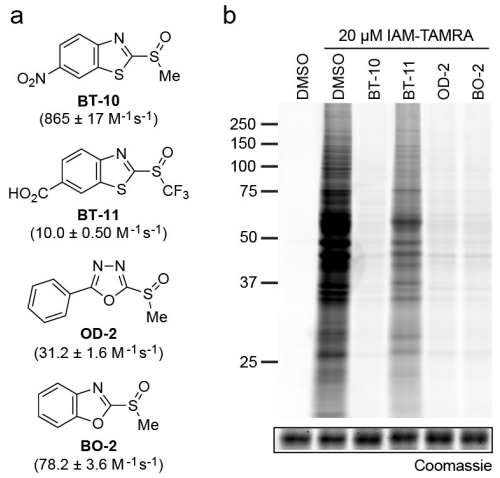


**Figure 4.** Heteroaromatic methyl sulfoxides are attenuated cysteine electrophiles. (a) Structures of heteroaromatic methyl sulfoxide analogues evaluated. Measured reaction rates are shown in parentheses below each electrophile. Standard deviations are derived from replicates with multi-point curve-fitting. (b) Competitive IAM-TAMRA activity-based profiling of cysteine electrophiles (5 mM) by in-gel fluorescence.

**Heteroaromatic sulfone stability in physiological buffer**. In comparison with NEM-cysteine conjugates, heteroaromatic–cysteine[2a] and heteroaromatic–selenocysteine[6b] conjugates demonstrate superior stability with no observable hydrolysis or reversibility. However, the stability of unconjugated heteroaromatic sulfones in aqueous buffers has not been reported. Therefore, we sought to establish any correlation between the observed reactivity across different heterocyclic classes of heteroaromatic sulfones with their stability. Nine different electrophiles were profiled in phosphate-buffered saline (PBS) at pH 7.4 under ambient conditions for 4 and 24 h by HPLC (**Figure S2**). Based on its material safety data sheet, iodoacetamide is light-sensitive, unstable, and requires fresh preparation at the time of use.[22] In contrast, we found IAM to be quite stable in PBS over 24 h. On the other hand, only ~50% of NEM was intact after 4 h. In agreement with their enhanced reactivity, **OD-1** and **BO-1** were the least stable heteroaromatic sulfones, undergoing considerable hydrolysis in the aqueous solution over 24 h. Therefore, disparate reports of **OD-1** reactivity are likely explained by a decomposed aliquot[2]. Interestingly, solid **BO-1** was completely decomposed after 6 months storage at –20 °C, while solid **OD-1** was stable under similar conditions for at least a year. In addition, benzothiazole and tetrazole methyl sulfones were remarkably stable in PBS. Even though its reaction rate is comparable to NEM, **BT-5** maintained exceptionally high stability. In fact, the aqueous solution of **Tz-1** and **BT-4** were benchtop stable for more than a week (data not shown), demonstrating robust properties for long-term storage. Altogether, the heterocyclic ring scaffolds contribute to the inherent stability of these compounds.

**Mass spectrometry-based proteomics with heteroaromatic sulfones.** IAM is the primary alkylation reagent used to prevent mixed disulfide formation in proteomics applications. Typical bottom-up proteomics workflows reduce protein samples with TCEP or DTT, followed by addition of excess (>20 mM) freshly prepared IAM.[23] Based on the accelerated rate constants and robust stability of new analogues, we selected IAM, NEM, and several heteroaromatic sulfone probes for in-depth, unenriched mass spectrometry profiling.

Mouse brain soluble proteome was heat-denatured, reduced with TCEP, and incubated with different probes for 30 minutes. The mixture was then digested with trypsin and analyzed by high resolution liquid chromatography mass spectrometry (LC-MS). Even without any enrichment, a short 2 h gradient yielded >3000 unique cysteine-modified peptides in duplicate analyses (**Tables 1 and S1**). While the number of unique cysteine-modified peptides identified for IAM was similar to **BT-4**, both **OD-1** and **Tz-1** yielded more labeled cysteine peptides. Conversely, combined analysis of both ring-opened and ring-closed NEM yielded significantly fewer cysteine-modified peptides than the other electrophiles. Overall, even without enrichment, this analysis identified >3000 peptides for each electrophile in a 2 h LC-MS experiment and ~6600 unique peptides pooled across different electrophiles. This finding suggests leveraging electrophile orthogonality can enhance cysteine coverage.

**Table 1**. Unenriched one-dimensional LC-MS proteomic evaluation of optimized heteroaromatic sulfones in mouse brain soluble proteome. The number of unique peptides from replicate analysis (N = 2) are listed. Peptides identified as deamidated, oxidized, or with different charge states are counted as one unique peptide. Lysine-modified peptides represent 1% or less of the total annotated peptides, or equivalent to assigned peptide false-discovery rate.[24]

| Electrophile | Unique proteins | Unique peptides | Cys-modified peptides | Lys-modified peptides |
|---|---|---|---|---|
| none | 3171 | 21116 | 0 | 0 |
| IAM | 3217 | 21602 | 3354 | 79 |
| NEM | 2990 | 20020 | 2620 | 201 |
| **Tz-1** | 3170 | 22348 | 3709 | 121 |
| **OD-1** | 3148 | 21909 | 3939 | 302 |
| **BT-4** | 3253 | 21764 | 3213 | 90 |

In addition, the ratios of annotated cysteine to annotated lysine labeled peptides for **Tz-1, BT-4**, and IAM were 30–42-fold. Conversely, the ratio for maleimide and **OD-1** only reached 13, suggesting reduced selectivity. Importantly, gel-based competitive analysis with NHS-TAMRA did not reveal any significant competition (**Figure S3**), implying the annotated sites are either highly abundant, exhibit high reactivity, or reflect false positives assigned within the 1% false-discovery rate.

Despite the dramatically disparate reaction rates, the number of modified peptides identified are similar across different electrophiles at these labeling concentrations. Interestingly, just 1.5 mM iodoacetamide (rather than >20 mM) was sufficient to alkylate >95% of cysteines across the proteome. Presumably, the remaining <5% are unreactive or inaccessible even in the presence of highly reactive electrophiles. To our surprise, different electrophiles reported a distinct, yet reproducible subset of

cysteine peptides (**Figure S4**). Different probes reported only ~55% overlap in peptide coverage. Since 81±1% of cysteine-peptides overlapped between runs within the same sample group, the observed orthogonality is unlikely derived from sample variation. Instead, the orthogonality is more likely attributed to shifts to less complex chromatographic windows (**Figure 5a**) or differences in fragmentation, which can directly influence peptide assignment. The elution profile for IAM overlaps more closely with unmodified peptides, while Tz, OD, and BT elute significantly later in the chromatographic gradient, potentially shifting their analysis away from peptide-dense elution times. This effect would increase the probability of data-dependent ion selection and improve ion purity (reduce co-isolation) to enhance peptide assignment.

It is also possible that different electrophiles have less beneficial electrospray ionization properties, which could impact detection of conjugated peptides. By averaging the ion current across commonly identified peptides, we derived a relative electrospray efficiency for each probe. Maleimide showed the weakest mean ion current, which likely contributes to the lower conjugate-peptide annotations. Otherwise, the relative electrospray ionization of heteroaromatic sulfone probes equaled or out-performed IAM (**Figure 5b**), further validating their expanded utility in proteomics applications.

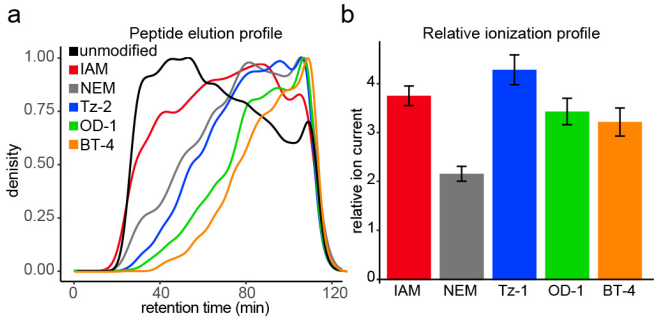


**Figure 5.** Electrophile profiling for optimal LC-MS analysis. (a) Right-shifted reversed-phase elution of heteroaromatic-labeled cysteine peptides. (b) Ion current intensity profile of labeled cysteine-peptides compared to matching unmodified peptides.

**Labeling cysteines in live cells.** Given their drug-like properties, we next evaluated heteroaromatic sulfone cell permeability and cysteine alkylation in live cultured HeLa cells. Alkyne-conjugated probes were synthesized to perform live cell cysteine alkylation, followed by cell lysis, click chemistry, and in-gel detection. These tools provide a modular platform for TOP-ABPP enrichment and site-specific analysis. IAM-Alkyne, Tz-Alkyne, and BT-Alkyne retained similar reaction rates as their parent electrophile, whereas the rate of OD-alkyne was 3-fold lower (**Figure 6a**), likely influenced by the less electronically favorable ether. Since the carboxylic acid of OD- and BO- probes were too unstable to purify, OD-alkyne employs a propargyl ether linkage with reduced reactivity.

*In situ* labeling was performed at three alkyne-probe concentrations (10, 30, and 100 µM) for 45 min in cysteine- and methionine-free Dulbecco's Modified Eagle Medium (DMEM). In this experiment, protein labeling occurs in direct competition with glutathione, cysteine and other thiol metabolites. At these lower labeling concentrations in HeLa cells, there was no noticeable morphological changes or cell death. After lysis, cell lysates were conjugated to TAMRA-azide for in-gel cysteine profiling (**Figure 6b**).

As expected, addition of 100 µM probe to cells yielded the highest labeling, albeit with subtle differences in the profile of labeled proteins. Unique labeling profiles were observed at lower probe concentrations in mouse brain soluble proteome, which may better represent differences across the most reactive cysteines (**Figure S5**). Despite large differences in reactivity, Tz-alkyne and BT-alkyne achieved similar intracellular labeling at equivalent concentrations. IAM also achieved relatively robust labeling, even though it is much less reactive than other probes. Presumably, the most reactive thiols are not greatly influenced by changes in probe electrophilicity. In addition, OD-alkyne achieved the lowest labeling in live cells, presumably due to its poor solubility and/or accelerated hydrolysis in aqueous media. Based on this analysis, solubility and cell permeability play important roles in the efficiency of intracellular cysteine labeling.

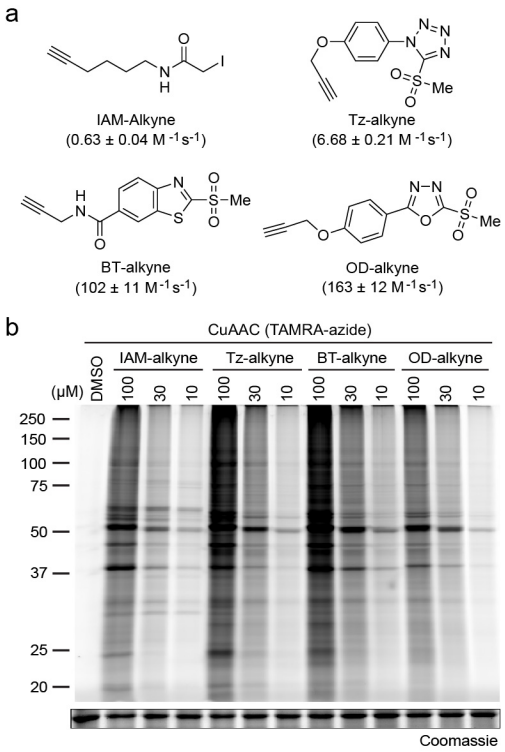


**Figure 6.** Live-cell cysteine labeling with alkyne-conjugated heteroaromatic sulfones. (a) Structures of alkyne-conjugated probes evaluated. Measured reaction rates are shown in parentheses below each electrophile. Standard deviations are derived from replicates with multi-point curve-fitting. (b) Concentration-dependent activity-based profiling of cysteine-labeling in HeLa cells. Visualized by in-gel fluorescence following click chemistry to TAMRA-azide.

**Site of labeling analysis.** Typical TOP-ABPP analysis sample preparation is manually intensive, involving extensive click chemistry steps, washes, and TEV cleavage prior to LC-MS analysis[14a]. Peptides are then analyzed across at least 5 separate fractions, totaling >10 h of instrument analysis time. Recent studies report cysteine peptide coverage anywhere from 800 to 5000 labeled cysteine peptides[13b, 25]. Alternatively, IAM-desthiobiotin enabled directed enrichment and detection of ~2700 cysteine-labeled peptides in cell lysates when analyzed across a short, 60 min LC-MS experiment[26]. A recent comparative analysis confirmed IAM-desthiobiotin achieves comparable cysteine coverage while shortening the sample preparation workflow by >1 day.[27] Offline fractionation and analysis of 7-

fractions by mass spectrometry further increased cysteine coverage >5-fold. These improvements dramatically expand proteome-wide assessment of cysteine occupancy while reducing the extended sample preparation time and technical error.[28] Based on these reports, click chemistry and orthogonal proteolysis are dispensable for profiling functional cysteines in complex lysates.

Accordingly, bypassing click chemistry labeling and cleavable linkers would be expected to streamline and enhance cysteine analysis. In order to explore this direct labeling and elution strategy, we synthesized BT-desthiobiotin-1 (**BT-D1**) (**Figure 7a**). **BT-D1** was incubated with live HeLa cells in cystine- and methionine-free DMEM. Analysis of the resulting lysate found near-saturated cysteine labeling within 5 minutes (**Figure 7b**). Nonetheless, initial mass spectrometry analysis in mouse brain soluble proteome reported widespread methyl ester hydrolysis in cells (**Table S2**). To avoid the additional complexity introduced by ester hydrolysis, a second-generation desthiobiotin analogue was synthesized, BT-desthiobiotin-2 **(BT-D2)** with a mono-PEG linker with equivalent cysteine reactivity. Both **BT-D1** and **BT-D2** showed reductions in cysteine reactivity compared to **BT-4**, likely introduced by the excess steric bulk of the desthiobiotin conjugate, yet still achieved 35-40-times greater reactivity than IAM-desthiobiotin (**IAM-D**).

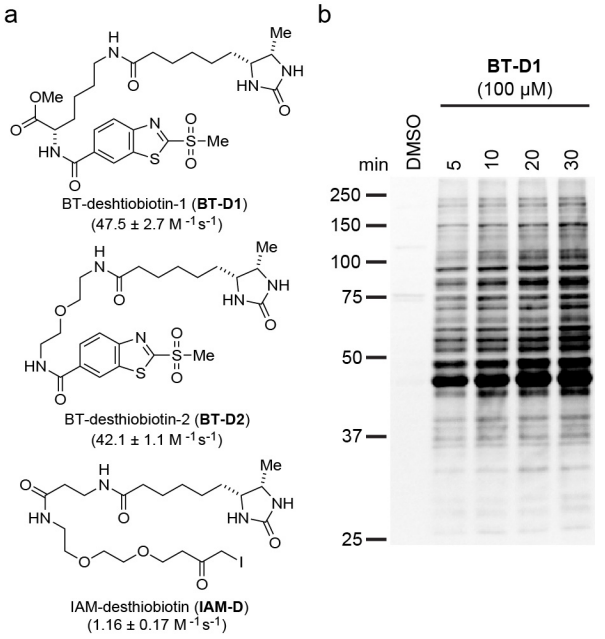


**Figure 7.** Rapid live cell cysteine labeling with desthiobiotin-linked probes. (a) Structures of desthiobiotin probes evaluated. Measured reaction rates are shown in parentheses below each electrophile. Standard deviations are derived from replicates with multi-point curve-fitting. (b) Streptavidin detection of time-dependent activity-based profiling in live HeLa cells.

HeLa cells were then incubated with either **BT**- or IAM-desthiobiotin probes for 1 h to evaluate in-cell cysteine profiles. Following heat denaturation, TCEP reduction, and alkylation with **BT-4** to block free thiols, the lysates were digested with trypsin and enriched with streptavidin resin. The eluted peptides were analyzed with a 2 h gradient by mass spectrometry. In total, this workflow yielded >3000 unique cysteine-labeled peptides profiled within their native cellular environment (**Figure 8 and Table S2**). Despite similar chromatographic elution profiles (**Figure 8a**) and peptide yields, only ~50% of the annotated peptides were common across both **BT**- and IAM-desthiobiotin probes (**Figure 8b**). These findings further corroborate orthogonality between different probe scaffolds in proteomic analysis. Altogether, the combined coverage pooling both **BT**- and IAM-desthiobiotin probes annotated ~5000 cysteine peptides engaged in live cells. In comparison, incubation for 1 h with 200 μM photo-caged IAM-alkyne probe in live HeLa cells detected ~1300 cysteines.[29]

Although heteroaromatic sulfones have been shown to be exclusively selective for cysteine over other nucleophilic amino acids such as lysine, serine, histidine, and tyrosine in THF/PBS (1:1) at room temperature[2a], their selectivity in the proteome under biological conditions have not been demonstrated. Here we corroborate these findings in live cells. Labeling was highly selective towards cysteine, with marginal identifications on other conjugated amino acids below the peptide false-discovery rate (**Figure S6**).[24]

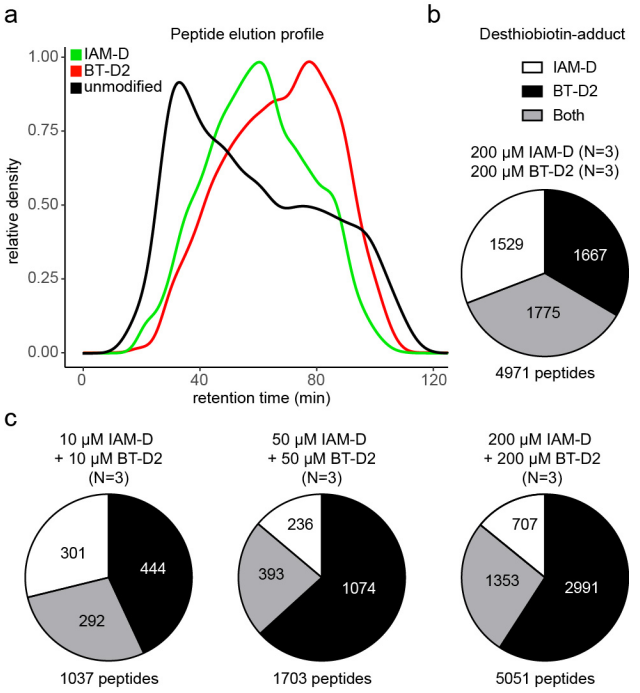


**Figure 8.** Orthogonal cysteine labeling with BT-desthiobiotin in live HeLa cells. (a) Equivalent reversed-phase elution of IAM-D, **BT-D1**, and **BT-D2** modifications of cysteine peptides. (b) Profile of annotated cysteine-conjugated peptides by LC-MS from separate (N=3) analyses of BT- and IAM-desthiobiotin labeled peptides. (c) In-cell competition of BT- and IAM-desthiobiotin probes. Peptides identified as deamidated, oxidized, or with different charge states are counted as one unique peptide.

In order to further evaluate in-cell labeling rates, we mixed both **BT**- and IAM-desthiobiotin probes simultaneously at three different concentrations (10, 50, or 200 μM) and added to live HeLa cells. Since, the reaction rate for **BT-D2** is ~36x faster than **IAM-D**, all three competition experiments yielded a greater number of **BT-D2** labeled cysteine peptides (**Figure 8c**, **Figure S7**, and **Table S2**). Prior to cysteine saturation at 10 μM, both **BT**- and IAM-desthiobiotin probes yield equivalent numbers of cysteine peptides. At 50 μM each probe, **BT-D2** begins to dominate the peptide identifications, presumably through direct competition with reactive and/or accessible thiols. At the highest concentration, **BT-D2** annotated nearly 3000 unique labeled peptides, with an additional ~1300 peptides in common

across both probes. Importantly, combining both **BT**- and IAM-desthiobiotin probes to cells simultaneously achieves >5000 annotated cysteine peptides, labeled in live cells, using a simplified 2 h LC-MS analysis. Therefore, co-incubating cells with more than one electrophile enhances cysteine-peptide coverage in a complex peptide analysis.

Importantly, even after increasing the probe concentrations, hundreds of peptides remained exclusive for a single probe. These differences do not appear to reflect steric differences, since established active site cysteines, including GAPDH, cystatin-B, thioredoxin, and phosphoglycerate dehydrogenase are modified by both probes across each tested concentration. There was also no clear difference in GO term identifiers between probes, suggesting little or no intrinsic chemical orthogonality (**Figure S8**). Interestingly, similar orthogonality was observed with ethynyl benziodoxolone (EBX) reagents, which report only fractional overlap (2/3) with iodoacetamide-based probes, suggesting physiochemical differences directly influence peptide-conjugate analysis.[30]

**Conclusions.** Maleimide remains the primary cysteine bioconjugation reagent, despite significant reversibility[31], ring hydrolysis[32], and non-specific reactivity[33] These issues are absent from heteroaromatic sulfones, which form stable adducts with cysteine[3]. Despite their promise, the reactivity and biological utility of heteroaromatic sulfones have not been thoroughly explored. Here we report a suite of analogues that define the structural-activity relationship for cysteine conjugation across several privileged heteroaromatic scaffolds. These analogues reveal synthetically accessible reactive centers capable of precise reactivity tuning. This includes modulating the sulfide oxidation state, modification of the leaving group, heteroatom substitutions, or addition of electron withdrawing or electron donating groups. Current efforts in cysteine-directed covalent drug discovery predominantly accesses a subset of validated electrophiles (i.e. acrylamides and chloroacetamides) with few rational routes to modulate tunability[16, 34]. Incorporation of heteroaromatic sulfide electrophiles as covalent warheads offers the potential to optimize reactivity to match the nucleophilicity of a targeted cysteine. Altogether, these approaches present a simple scaffold able to span a wide range of reactivities by implementing only minimal chemical modifications.

In addition, we demonstrate both iodoacetamide and methylsulfonylbenzothiazole desthiobiotin probes achieve live cell cysteine engagement and direct enrichment without the need for further click chemistry conjugation. These reagents provide a simplified method to directly profile cellular thiols in their native environment without lysis and exposure to atmospheric oxygen or disruption of multi-protein complexes. By direct profiling of native thiols in live cells, druggable sites can be assayed for target engagement in cells using competitive ABPP methods. Such in-cell assays provide a critical link between druggable cysteine discovery in lysates and validation in live cells, particularly with emerging bifunctional covalent ligands for targeted protein degradation.[35]

Finally, optimized heteroaromatic sulfones provide accelerated reaction kinetics to afford more precise temporal control of cysteine alkylation in live cells. These tools promise to enable direct evaluation of cysteine oxidation at much shorter time scales with improved selectivity within their native subcellular environment[2b]. Furthermore, the more non-polar probes provide a privileged route to directly profile cysteines in more hydrophobic environments, such as sites of *S*-palmitoylation. Overall, these probes offer a chemically tractable alternative for tunable cysteine conjugation and in-depth cellular profiling.

## ASSOCIATED CONTENT

### Supporting Information

The Supporting Information is available free of charge on the ACS Publications website.

Synthetic methods and characterization. Supporting figures S1-S8 including electrophile titrations, stability, lysine reactivity, click chemistry gel analysis, and comparative proteomics analysis. (PDF)
Combined mouse brain proteomics data, Table S1. (XLSX)
Combined site-specific desthiobiotin-probe proteomics data, Table S2. (XLSX)

## AUTHOR INFORMATION

### Corresponding Author

*brentrm@umich.edu

### Funding Sources

Financial support was provided by the National Institutes of Health DP2 GM114848 (B.R.M) and the University of Michigan. Mass spectrometry instrumentation was supported by the National Institute of Health S10 OD021619.

## ACKNOWLEDGMENT

We thank John E. Crellin (Michigan) for initial chemical synthesis, Sarah Haynes (Michigan) and Jaimeen Majmudar (Pfizer) for assisting with proteomics data analysis, and Gabriela Gregorian (Michigan) for mass spectrometry support.

## REFERENCES

1. Zhang, D.; Devarie-Baez, N. O.; Li, Q.; Lancaster, J. R., Jr.; Xian, M., Methylsulfonyl benzothiazole (MSBT): a selective protein thiol blocking reagent. Org. Lett. 2012, 14 (13), 3396-9.

2. (a) Toda, N.; Asano, S.; Barbas, C. F., 3rd, Rapid, stable, chemoselective labeling of thiols with Julia-Kocienski-like reagents: a serum-stable alternative to maleimide-based protein conjugation. Angew. Chem., Int. Ed. 2013, 52 (48), 12592-6; (b) Chen, X.; Wu, H.; Park, C. M.; Poole, T. H.; Keceli, G.; Devarie-Baez, N. O.; Tsang, A. W.; Lowther, W. T.; Poole, L. B.; King, S. B.; Xian, M.; Furdui, C. M., Discovery of Heteroaromatic Sulfones As a New Class of Biologically Compatible Thiol-Selective Reagents. ACS Chem. Biol. 2017, 12 (8), 2201-2208.

3. Patterson, J. T.; Asano, S.; Li, X.; Rader, C.; Barbas, C. F., 3rd, Improving the serum stability of site-specific antibody conjugates with sulfone linkers. Bioconjugate Chem. 2014, 25 (8), 1402-7.

4. Reisz, J. A.; Bechtold, E.; King, S. B.; Poole, L. B.; Furdui, C. M., Thiol-blocking electrophiles interfere with labeling and detection of protein sulfenic acids. FEBS J. 2013, 280 (23), 6150-61.

5. (a) Gill, R. K.; Rawal, R. K.; Bariwal, J., Recent Advances in the Chemistry and Biology of Benzothiazoles. Arch. Pharm. 2015, 348 (3), 155-178; (b) Davinder, K.; Virender, K.; Rakesh Marwaha and Gajendra, S., Oxadiazole-An Important Bioactive Scaffold for Drug Discovery and Development Process Against HIV and Cancer- A Review. Curr. Bioact. Compd. 2019, 15 (3), 271-279; (c) Sharma, P. C.; Sinhmar, A.; Sharma, A.; Rajak, H.; Pathak, D. P., Medicinal significance of benzothiazole scaffold: an insight view. J. Enzyme Inhib. Med. Chem. 2013, 28 (2), 240-266; (d) Myznikov, L. V.; Hrabalek, A.; Koldobskii, G. I., Drugs in the tetrazole series. (Review). Chem. Heterocycl. Compd. 2007, 43 (1), 1-9; (e) Ostrovskii, V. A.; Trifonov, R. E.; Popova, E. A., Medicinal chemistry of tetrazoles. Russ. Chem. Bull. 2012, 61 (4), 768-780; (f) Velík, J.; Baliharová, V.; Fink-Gremmels, J.; Bull, S.; Lamka, J.; Skálová, L., Benzimidazole drugs and modulation of biotransformation enzymes. Res. Vet. Sci. 2004, 76 (2), 95-108; (g)

Musmade, D. S.; Pattan, S. R.; Yalgatti, M. S., Oxadiazole a nucleus with versatile biological behaviour. Int. J. Pharm. Chem. 2015, 5 (1), 11-20.

6. (a) Farrukh, A.; Paez, J. I.; Salierno, M.; del Campo, A., Bioconjugating Thiols to Poly(acrylamide) Gels for Cell Culture Using Methylsulfonyl Co-monomers. Angew. Chem., Int. Ed. 2016, 55 (6), 2092-2096; (b) Pedzisa, L.; Li, X.; Rader, C.; Roush, W. R., Assessment of reagents for selenocysteine conjugation and the stability of selenocysteine adducts. Org. Biomol. Chem. 2016, 14 (22), 5141-5147.

7. Bueno, A. B.; Showalter, A. D.; Wainscott, D. B.; Stutsman, C.; Marin, A.; Ficorilli, J.; Cabrera, O.; Willard, F. S.; Sloop, K. W., Positive Allosteric Modulation of the Glucagon-like Peptide-1 Receptor by Diverse Electrophiles. J. Biol. Chem. 2016, 291 (20), 10700-15.

8. Chen, B.; Long, Q.; Zhao, Y.; Wu, Y.; Ge, S.; Wang, P.; Yang, C.-G.; Chi, Y.; Song, B.; Yang, S., Sulfone-Based Probes Unraveled Dihydrolipoamide S-Succinyltransferase as an Unprecedented Target in Phytopathogens. J. Agric. Food Chem. 2019, 67 (25), 6962-6969.

9. (a) Lad, N. P.; Manohar, Y.; Mascarenhas, M.; Pandit, Y. B.; Kulkarni, M. R.; Sharma, R.; Salkar, K.; Suthar, A.; Pandit, S. S., Methylsulfonyl benzothiazoles (MSBT) derivatives: Search for new potential antimicrobial and anticancer agents. Bioorganic & Medicinal Chemistry Letters 2017, 27 (5), 1319-1324; (b) Xu, W.; Yang, S.; Bhadury, P.; He, J.; He, M.; Gao, L.; Hu, D.; Song, B., Synthesis and bioactivity of novel sulfone derivatives containing 2,4-dichlorophenyl substituted 1,3,4-oxadiazole/thiadiazole moiety as chitinase inhibitors. Pestic. Biochem. Physiol. 2011, 101 (1), 6-15; (c) Su, S.; Zhou, X.; Zhou, Y.; Liao, G.; Shi, L.; Yang, X.; Zhang, X.; Jin, L., Synthesis and Biological Evaluation of Novel Sulfone Derivatives Containing 1,3,4-Oxadiazole Moiety. World J. Org. Chem. 2014, 2 (1), 18-27.

10. Bauer, M. R.; Joerger, A. C.; Fersht, A. R., 2-Sulfonylpyrimidines: Mild alkylating agents with anticancer activity toward p53-compromised cells. Proc. Natl. Acad. Sci. U. S. A. 2016, 113 (36), E5271-80.

11. Coulson, G. B.; Johnson, B. K.; Zheng, H.; Colvin, C. J.; Fillinger, R. J.; Haiderer, E. R.; Hammer, N. D.; Abramovitch, R. B., Targeting Mycobacterium tuberculosis Sensitivity to Thiol Stress at Acidic pH Kills the Bacterium and Potentiates Antibiotics. Cell Chem. Biol. 2017, 24 (8), 993-1004 e4.

12. Kahl, D. J.; Hutchings, K. M.; Lisabeth, E. M.; Haak, A. J.; Leipprandt, J. R.; Dexheimer, T.; Khanna, D.; Tsou, P. S.; Campbell, P. L.; Fox, D. A.; Wen, B.; Sun, D.; Bailie, M.; Neubig, R. R.; Larsen, S. D., 5-Aryl-1,3,4-oxadiazol-2-ylthioalkanoic Acids: A Highly Potent New Class of Inhibitors of Rho/Myocardin-Related Transcription Factor (MRTF)/Serum Response Factor (SRF)-Mediated Gene Transcription as Potential Antifibrotic Agents for Scleroderma. J .Med. Chem. 2019, 62 (9), 4350-4369.

13. (a) Qian, Y.; Weerapana, E., A Quantitative Mass-Spectrometry Platform to Monitor Changes in Cysteine Reactivity. Methods Mol. Biol. 2017, 1491, 11-22; (b) Weerapana, E.; Wang, C.; Simon, G. M.; Richter, F.; Khare, S.; Dillon, M. B.; Bachovchin, D. A.; Mowen, K.; Baker, D.; Cravatt, B. F., Quantitative reactivity profiling predicts functional cysteines in proteomes. Nature 2010, 468 (7325), 790-5.

14. (a) Weerapana, E.; Speers, A. E.; Cravatt, B. F., Tandem orthogonal proteolysis-activity-based protein profiling (TOP-ABPP)--a general method for mapping sites of probe modification in proteomes. Nat. Protoc. 2007, 2 (6), 1414-25; (b) Speers, A. E.; Cravatt, B. F., A tandem orthogonal proteolysis strategy for high-content chemical proteomics. J. Am. Chem. Soc. 2005, 127 (28), 10018-9.

15. Zhou, Y.; Wynia-Smith, S. L.; Couvertier, S. M.; Kalous, K. S.; Marletta, M. A.; Smith, B. C.; Weerapana, E., Chemoproteomic Strategy to Quantitatively Monitor Transnitrosation Uncovers Functionally Relevant S-Nitrosation Sites on Cathepsin D and HADH2. Cell Chem. Biol. 2016, 23 (6), 727-37.

16. Backus, K. M.; Correia, B. E.; Lum, K. M.; Forli, S.; Horning, B. D.; Gonzalez-Paez, G. E.; Chatterjee, S.; Lanning, B. R.; Teijaro, J. R.; Olson, A. J.; Wolan, D. W.; Cravatt, B. F., Proteome-wide covalent ligand discovery in native biological systems. Nature 2016, 534 (7608), 570-4.

17. Yang, F.; Gao, J.; Che, J.; Jia, G.; Wang, C., A Dimethyl-Labeling-Based Strategy for Site-Specifically Quantitative Chemical Proteomics. Anal Chem 2018, 90 (15), 9576-9582.

18. (a) Bar-Peled, L.; Kemper, E. K.; Suciu, R. M.; Vinogradova, E. V.; Backus, K. M.; Horning, B. D.; Paul, T. A.; Ichu, T. A.; Svensson, R. U.; Olucha, J.; Chang, M. W.; Kok, B. P.; Zhu, Z.; Ihle, N. T.; Dix, M. M.; Jiang, P.; Hayward, M. M.; Saez, E.; Shaw, R. J.; Cravatt, B. F., Chemical Proteomics Identifies Druggable Vulnerabilities in a Genetically Defined Cancer. Cell 2017, 171 (3), 696-709 e23; (b) Grossman, E. A.; Ward, C. C.; Spradlin, J. N.; Bateman, L. A.; Huffman, T. R.; Miyamoto, D. K.; Kleinman, J. I.; Nomura, D. K., Covalent Ligand Discovery against Druggable Hotspots Targeted by Anticancer Natural Products. Cell Chem. Biol. 2017, 24 (11), 1368-1376 e4.

19. Chiotellis, A.; Sladojevich, F.; Mu, L.; Müller Herde, A.; Valverde, I. E.; Tolmachev, V.; Schibli, R.; Ametamey, S. M.; Mindt, T. L., Novel chemoselective 18F-radiolabeling of thiol-containing biomolecules under mild aqueous conditions. Chem. Commun. 2016, 52 (36), 6083-6086.

20. Hansch, C.; Leo, A.; Taft, R. W., A survey of Hammett substituent constants and resonance and field parameters. Chem. Rev. 1991, 91 (2), 165-195.

21. (a) Äbelö, A.; Andersson, T. B.; Antonsson, M.; Naudot, A. K.; Skånberg, I.; Weidolf, L., Stereoselective Metabolism of Omeprazole by Human Cytochrome P450 Enzymes. Drug Metab. Dispos. 2000, 28 (8), 966; (b) Lipsky, J. J., Mechanism of the inhibition of the gamma-carboxylation of glutamic acid by N-methylthiotetrazole-containing antibiotics. Proc. Natl. Acad. Sci. U. S. A. 1984, 81 (9), 2893.

22. Aitken, A.; Learmonth, M., Carboxymethylation of Cysteine Using Iodoacetamide/Iodoacetic Acid. In The Protein Protocols Handbook, Walker, J. M., Ed. Humana Press: Totowa, NJ, 1996; pp 339-340.

23. Suttapitugsakul, S.; Xiao, H.; Smeekens, J.; Wu, R., Evaluation and optimization of reduction and alkylation methods to maximize peptide identification with MS-based proteomics. Mol. BioSyst. 2017, 13 (12), 2574-2582.

24. Chalkley, R. J., When target-decoy false discovery rate estimations are inaccurate and how to spot instances. J Proteome Res 2013, 12 (2), 1062-4.

25. Senkane, K.; Vinogradova, E. V.; Suciu, R. M.; Crowley, V. M.; Zaro, B. W.; Bradshaw, J. M.; Brameld, K. A.; Cravatt, B. F., The Proteome-Wide Potential for Reversible Covalency at Cysteine. Angew. Chem., Int. Ed. 2019, 58 (33), 11385-11389.

26. Patricelli, M. P.; Janes, M. R.; Li, L. S.; Hansen, R.; Peters, U.; Kessler, L. V.; Chen, Y.; Kucharski, J. M.; Feng, J.; Ely, T.; Chen, J. H.; Firdaus, S. J.; Babbar, A.; Ren, P.; Liu, Y., Selective Inhibition of Oncogenic KRAS Output with Small Molecules Targeting the Inactive State. Cancer Discovery 2016, 6 (3), 316-29.

27. Zanon, P. R. A.; Lewald, L.; Hacker, S. M., Isotopically Labeled Desthiobiotin Azide (isoDTB) Tags Enable Global Profiling of the Bacterial Cysteinome. Angew. Chem. Int. Ed. Engl. 2019.

28. Vinogradova, E. V.; Lazar, D. C.; Suciu, R. M.; Wang, Y.; Bianco, G.; Yamashita, Y.; Crowley, V. M.; Remillard, D.; Lum, K. M.; Simon, G. M.; Kemper, E. K.; Lazear, M. R.; Yin, S.; Blewett, M. M.; Dix, M. M.; Nguyen, N.; Shokhirev, M. N.; Chin, E.; Lairson, L.; Forli, S.; Teijaro, J. R.; Cravatt, B. F., An activity-guided map of electrophile-cysteine interactions in primary human immune cells. bioRxiv 2019, 808113.

29. Abo, M.; Bak, D. W.; Weerapana, E., Optimization of Caged Electrophiles for Improved Monitoring of Cysteine Reactivity in Living Cells. ChemBioChem 2017, 18 (1), 81-84.

30. Abegg, D.; Frei, R.; Cerato, L.; Prasad Hari, D.; Wang, C.; Waser, J.; Adibekian, A., Proteome-Wide Profiling of Targets of Cysteine reactive Small Molecules by Using Ethynyl Benziodoxolone Reagents. Angew. Chem. Int. Ed. Engl. 2015, 54 (37), 10852-7.

31. Baldwin, A. D.; Kiick, K. L., Tunable degradation of maleimide-thiol adducts in reducing environments. Bioconjugate Chem. 2011, 22 (10), 1946-53.

32. Matsui, S.; Aida, H., Hydrolysis of some N-alkylmaleimides. J. Chem. Soc., Perkin Trans. 2 1978, (12), 1277-1280.

33. (a) Kuo, Y. H.; Konopko, A. M.; Borotto, N. B.; Majmudar, J. D.; Haynes, S. E.; Martin, B. R., Profiling Protein S-Sulfination with Maleimide-Linked Probes. ChemBioChem 2017, 18 (20), 2028-2032; (b) Zhang, Y.; Zhou, X.; Xie, Y.; Greenberg, M. M.; Xi, Z.; Zhou, C., Thiol Specific and Tracelessly Removable Bioconjugation via Michael Addition to 5-Methylene Pyrrolones. J. Am. Chem. Soc. 2017, 139 (17), 6146-6151; (c) Ravasco, J. M. J. M.; Faustino, H.; Trindade, A.; Gois, P. M. P., Bioconjugation with Maleimides: A Useful Tool for Chemical Biology. Chem.: Eur. J. 2019, 25 (1), 43-59.

34. Resnick, E.; Bradley, A.; Gan, J.; Douangamath, A.; Krojer, T.; Sethi, R.; Geurink, P. P.; Aimon, A.; Amitai, G.; Bellini, D.; Bennett, J.; Fairhead, M.; Fedorov, O.; Gabizon, R.; Gan, J.; Guo, J.; Plotnikov, A.; Reznik, N.; Ruda, G. F.; Diaz-Saez, L.; Straub, V. M.; Szommer, T.; Velupillai, S.; Zaidman, D.; Zhang, Y.; Coker, A. R.; Dowson, C. G.; Barr, H. M.; Wang, C.; Huber, K. V. M.; Brennan, P. E.; Ovaa, H.; von Delft, F.; London, N., Rapid Covalent-Probe Discovery by Electrophile-Fragment Screening. J. Am. Chem. Soc. 2019, 141 (22), 8951-8968.

35. (a) Spradlin, J. N.; Hu, X.; Ward, C. C.; Brittain, S. M.; Jones, M. D.; Ou, L.; To, M.; Proudfoot, A.; Ornelas, E.; Woldegiorgis, M.; Olzmann, J. A.; Bussiere, D. E.; Thomas, J. R.; Tallarico, J. A.; McKenna, J. M.; Schirle, M.; Maimone, T. J.; Nomura, D. K., Harnessing the anti-cancer natural product nimbolide for targeted protein degradation. Nat. Chem. Biol. 2019, 15 (7), 747-755; (b) Zhang, X.; Crowley, V. M.; Wucherpfennig, T. G.; Dix, M. M.; Cravatt, B. F., Electrophilic PROTACs that degrade nuclear proteins by engaging DCAF16. Nat. Chem. Biol. 2019, 15 (7), 737-746.

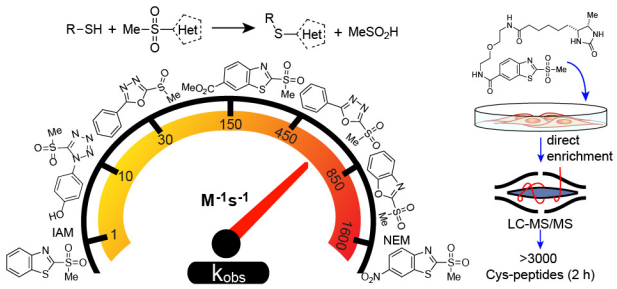
R–SH + Me–S(=O)2–Het
R–S–Het + MeSO2H
IAM
NEM
1
10
30
150
450
850
1600
M-1s-1
kobs
direct enrichment
LC-MS/MS
>3000
Cys-peptides (2 h)

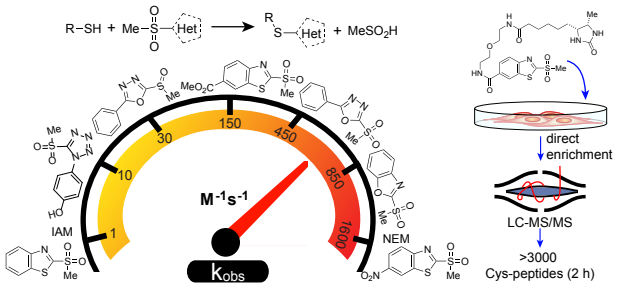
R–SH + Me–Het
R–Het + MeSO2H
1
10
30
150
450
820
1600
M-1s-1
kobs
IAM
NEM
direct enrichment
LC-MS/MS
>3000 Cys-peptides (2 h)

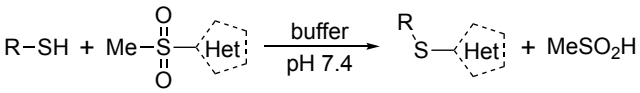
R–SH + Me–S(=O)(=O)–Het
buffer
pH 7.4
R–S–Het + MeSO2H

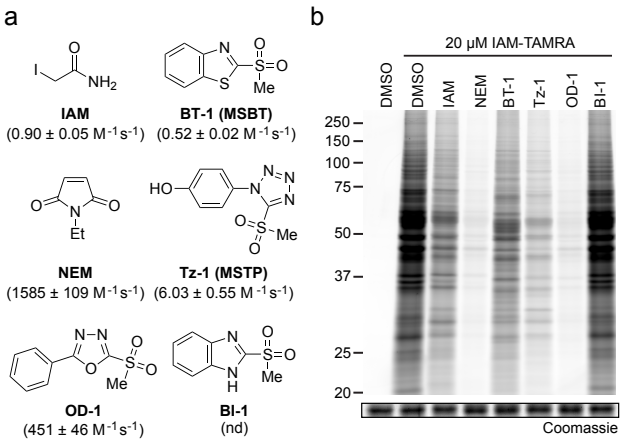
a
IAM
(0.90 ± 0.05 M-1s-1)
BT-1 (MSBT)
(0.52 ± 0.02 M-1s-1)
NEM
(1585 ± 109 M-1s-1)
Tz-1 (MSTP)
(6.03 ± 0.55 M-1s-1)
OD-1
(451 ± 46 M-1s-1)
BI-1
(nd)
b
20 μM IAM-TAMRA
DMSO
DMSO
IAM
NEM
BT-1
Tz-1
OD-1
BI-1
250
150
100
75
50
37
25
20
Coomassie

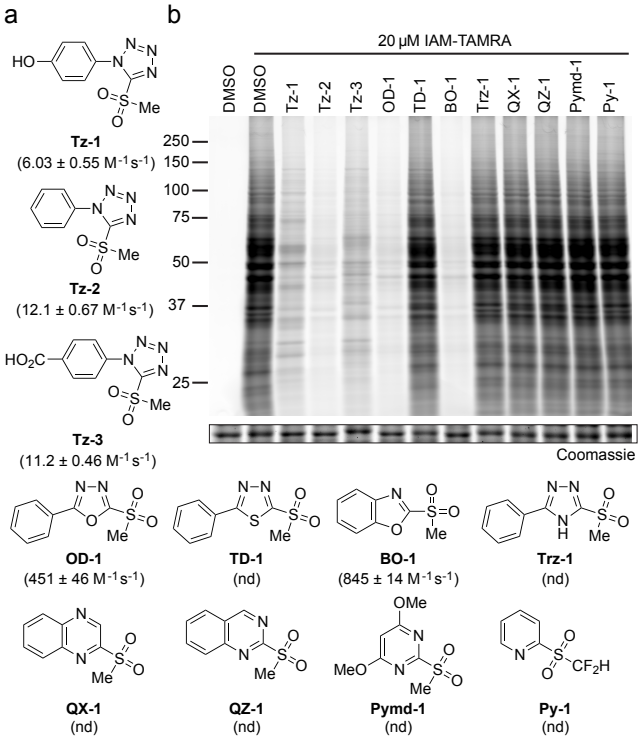
a
b
20 μM IAM-TAMRA
DMSO
DMSO
Tz-1
Tz-2
Tz-3
OD-1
TD-1
BO-1
Trz-1
QX-1
QZ-1
Pymd-1
Py-1
250
150
100
75
50
37
25
Coomassie
Tz-1
(6.03 ± 0.55 M-1s-1)
Tz-2
(12.1 ± 0.67 M-1s-1)
Tz-3
(11.2 ± 0.46 M-1s-1)
OD-1
(451 ± 46 M-1s-1)
TD-1
(nd)
BO-1
(845 ± 14 M-1s-1)
Trz-1
(nd)
QX-1
(nd)
QZ-1
(nd)
Pymd-1
(nd)
Py-1
(nd)

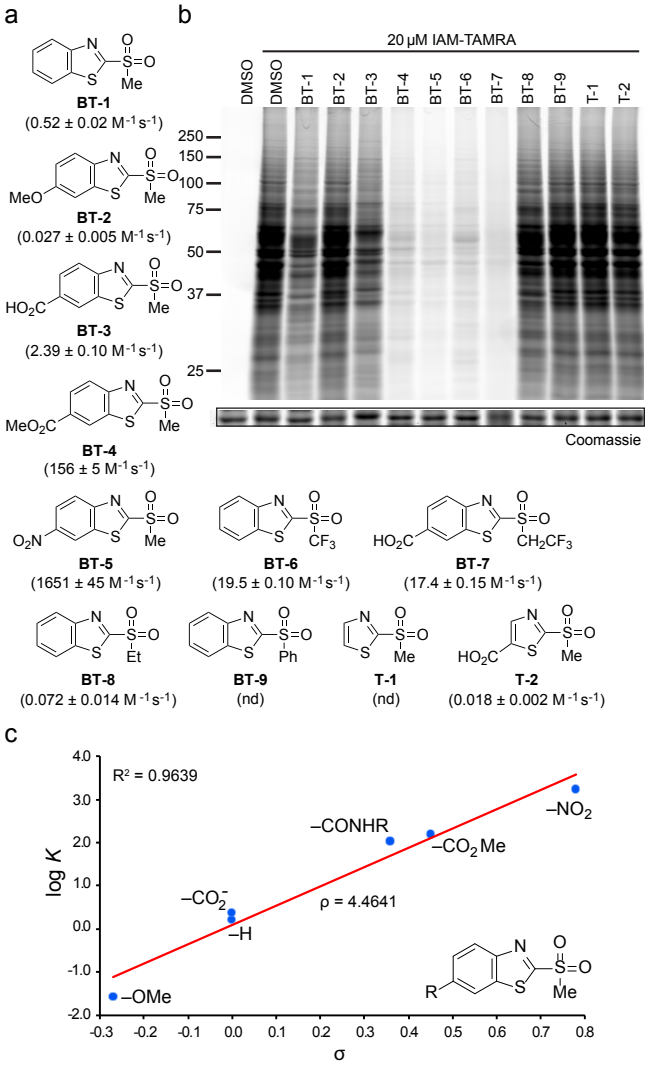
a
b
BT-1
(0.52 ± 0.02 M-1 s-1)
BT-2
(0.027 ± 0.005 M-1 s-1)
BT-3
(2.39 ± 0.10 M-1 s-1)
BT-4
(156 ± 5 M-1 s-1)
BT-5
(1651 ± 45 M-1 s-1)
BT-6
(19.5 ± 0.10 M-1 s-1)
BT-7
(17.4 ± 0.15 M-1 s-1)
BT-8
(0.072 ± 0.014 M-1 s-1)
BT-9
(nd)
T-1
(nd)
T-2
(0.018 ± 0.002 M-1 s-1)
20 μM IAM-TAMRA
DMSO
DMSO
BT-1
BT-2
BT-3
BT-4
BT-5
BT-6
BT-7
BT-8
BT-9
T-1
T-2
250
150
100
75
50
37
25
Coomassie
c
R² = 0.9639
ρ = 4.4641
log K
σ
–NO2
–CONHR
–CO2Me
–CO2-
–H
–OMe

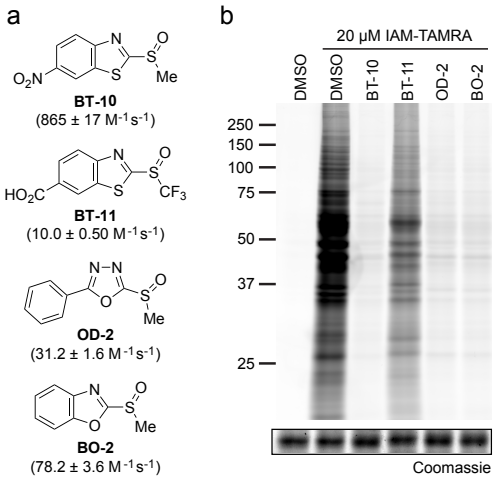
a
BT-10
(865 ± 17 M-1s-1)
BT-11
(10.0 ± 0.50 M-1s-1)
OD-2
(31.2 ± 1.6 M-1s-1)
BO-2
(78.2 ± 3.6 M-1s-1)
b
20 μM IAM-TAMRA
DMSO
DMSO
BT-10
BT-11
OD-2
BO-2
250
150
100
75
50
37
25
Coomassie

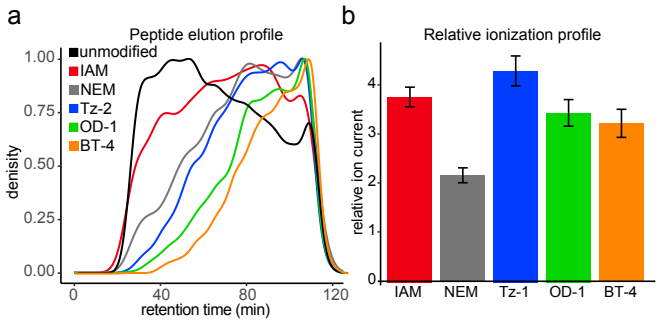
a
Peptide elution profile
unmodified
IAM
NEM
Tz-2
OD-1
BT-4
denisity
1.00
0.75
0.50
0.25
0.00
0
40
80
120
retention time (min)
b
Relative ionization profile
relative ion current
4
3
2
1
0
IAM
NEM
Tz-1
OD-1
BT-4

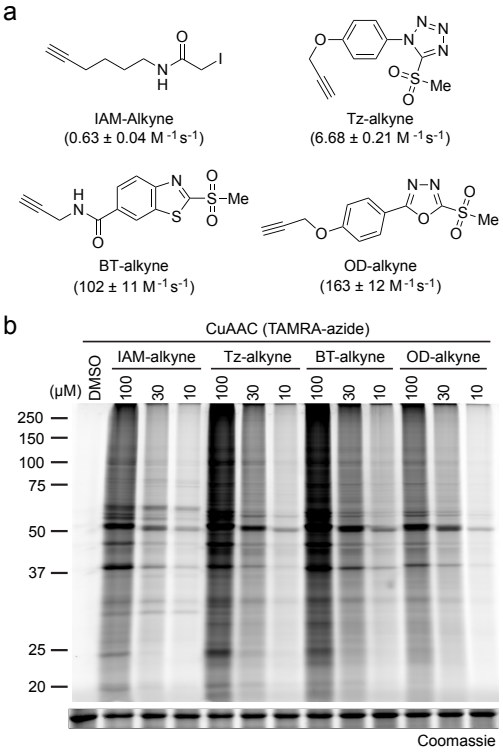
a
IAM-Alkyne
(0.63 ± 0.04 M -1s-1)
Tz-alkyne
(6.68 ± 0.21 M -1s-1)
BT-alkyne
(102 ± 11 M-1s-1)
OD-alkyne
(163 ± 12 M-1s-1)
b
CuAAC (TAMRA-azide)
DMSO
IAM-alkyne
Tz-alkyne
BT-alkyne
OD-alkyne
(μM)
100
30
10
250
150
100
75
50
37
25
20
Coomassie

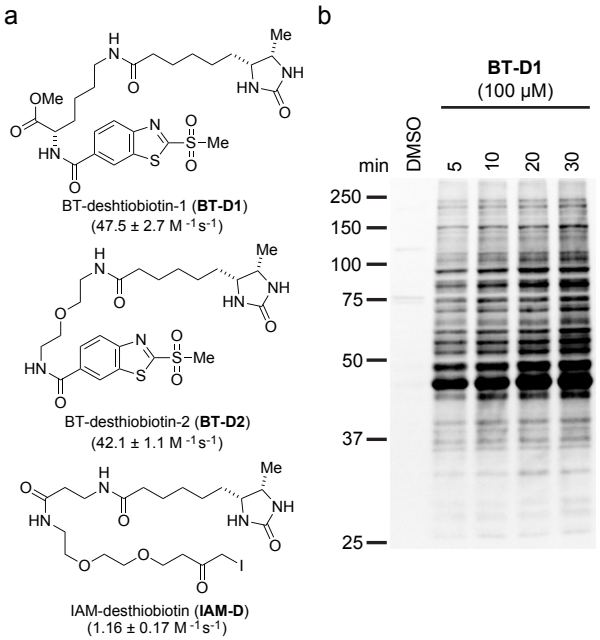
a
b
BT-deshtiobiotin-1 (BT-D1)
(47.5 ± 2.7 M -1s-1)
BT-desthiobiotin-2 (BT-D2)
(42.1 ± 1.1 M -1s-1)
IAM-desthiobiotin (IAM-D)
(1.16 ± 0.17 M -1s-1)
BT-D1
(100 μM)
DMSO
min
5
10
20
30
250
150
100
75
50
37
25

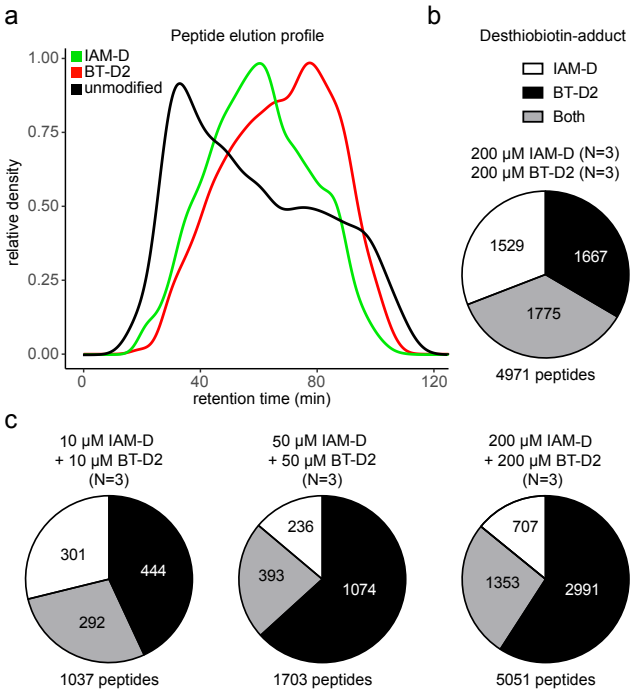
a
Peptide elution profile
IAM-D
BT-D2
unmodified
relative density
1.00
0.75
0.50
0.25
0.00
0
40
80
120
retention time (min)
b
Desthiobiotin-adduct
IAM-D
BT-D2
Both
200 µM IAM-D (N=3)
200 µM BT-D2 (N=3)
1529
1667
1775
4971 peptides
c
10 µM IAM-D
+ 10 µM BT-D2
(N=3)
301
444
292
1037 peptides
50 µM IAM-D
+ 50 µM BT-D2
(N=3)
236
393
1074
1703 peptides
200 µM IAM-D
+ 200 µM BT-D2
(N=3)
707
1353
2991
5051 peptides